Research Paper

Study on the Decrease in Neuronal Autophagy/Apoptosis by Fuyuan Xingnao Decoction in Rats with Cerebral Hemorrhage

MOYAN WANG, XUE BAI[1] AND BANGJIANG FANG[1,2]*

Department of Medicine, Institute of Integrated Chinese and Western Medicine, Southwest Medical University, Sichuan, Luzhou 646099, [1]Department of Neurology, National Traditional Chinese Medicine Clinical Research Base, The Affiliated Traditional Chinese Medicine Hospital, Southwest Medical University, Sichuan, Luzhou 646610, [2]Emergency Department, Longhua Hospital Affiliated to Shanghai University of Traditional Chinese Medicine, Shanghai, Xuhui 200032, China

The objective of this study was to investigate the effects of autophagy/apoptosis on neurons following cerebral hemorrhage in rats, specifically focusing on the regulation of B cell lymphoma-2 on B cell lymphoma-2 associated X, beclin-1 and the regulatory mechanism of autophagy/apoptosis by Fuyuan Xingnao decoction. Rapamycin and Fuyuan Xingnao decoction were used to treat neurons in rats that had cerebral hemorrhage as well as neurons that mimicked it; autophagy is agonistic to rapamycin. Following 3 d of brain bleeding, there was an increase in both autophagy and apoptosis. When rats with cerebral hemorrhage were given Fuyuan Xingnao decoction, autophagy and apoptosis increased and the neurological impairments were decreased. In contrast, rapamycin boosted these processes in the same animals. Fuyuan Xingnao decoction can preserve neurons in rats suffering from cerebral hemorrhage, decrease autophagy and apoptosis following cerebral hemorrhage thereby ameliorating the neurological impairments.

Key words: Cerebral hemorrhage, autophagy, apoptosis, Fuyuan Xingnao decoction, rapamycin

With over 2.8 million deaths annually, Intracerebral Hemorrhage (ICH) is a more deadly stroke condition than cerebral infarction[1]. The neurological deficits and longevity of survivors are of concern[2]; however, there is still no clear treatment for its root cause[1]. Autophagy occurs after ICH and is a common form of self-rescue, which increases the chances of survival through energy recycling and waste removal. Endoplasmic reticulum-induced autophagy contributes to apoptosis suppression in the early stages of ICH, but prolonged autophagy increases apoptosis after ICH[3].

According to Traditional Chinese Medicine (TCM), the essence of human illness lies in the weakness of human life force (positive qi) or inability to adapt to external changes (evil qi) while the essence of the disease for cerebral hemorrhage lies in the imbalance of yin and yang in the body, lack of positive qi. Fuyuan Xingnao (FYXN) uses *ginseng* to replenish positive qi and the rest of the medicinal flavors to remove the evil qi. The mechanism of FYXN in treating diabetes mellitus combined with cerebral infarction has been discovered in the past[4,5] but the mechanism of treating cerebral hemorrhage has not yet been elucidated.

B cell lymphoma-2 (Bcl-2) is a key factor of apoptosis, which can bind to Bcl-2 Associated X (BAX) protein to prevent the initiation of apoptosis and can also bind to Beclin-1 (BECN-1) to prevent autophagy[6]. The regulation of Jun N-terminal Kinase (JNK) can induce the dissociation of Bcl-2 from BECN-1, which regulates the autophagy mechanism[7]. FYXN helps to wake up the brain, by regulating autophagy/apoptosis after cerebral hemorrhage through JNK/Bcl-2. Continuous autophagy triggers apoptosis and FYXN may prevent apoptosis by reducing autophagy. This regulation may be related to Bcl-2 and to test this theory, we conducted the following experiments.

MATERIALS AND METHODS

In vivo experimental animals:

120 male Sprague-Dawley (SD) adult rats weighing around (250-300) g were purchased from the Experimental Animal Centre of Southwest Medical University (License No: SCXK (Chuan) 2018-17 and 065). 5 rats/cage were housed and the experiment was conducted at constant temperature of 25°±2°, by maintaining humidity of 50 %-55 %, light/dark cycle

***Address for correspondence**
E-mail: fangbji@163.com

for 12 h in a controlled and quiet environment with free access to food and water.

Preparation of FYXN decoction: FYXN originated in the preparation room of the Affiliated Hospital of TCM at Southwest Medical University, which was composed of *Acorus calamus, Panax notoginseng, Panax ginseng, Arisaema consanguineum* Schott, *Rheum officinale* Baill, *Leonurus heterophyllus* and leech; all the components were split up into 10:15:12:10:10:30:10 ratios[8]. The concentrate was made at a concentration of 2 g/ml, cleaned and refrigerated after the other herbs were decocted three times in water and the leftovers were removed. Among these, protein was extracted by soaking *ginseng* in 70 % ethanol for 1 w, while the volatile oil was obtained from *calamus*.

Experimental method:

62 healthy male SD adult rats weighing (250±50) g were obtained from the Southwest Medical University Laboratory Animal Center (Production No: SYXK (Chuan) 2023-0017 and License No: SYXK (Chuan) 2023-0065). In order to provide the rats with a stable and clean environment for rearing, 6 rats/cage were housed under Specific Pathogen Free (SPF) experimental conditions. Throughout the experiment, rats received *ad libitum* access to standard diet, clean and filtered water. Every surgical operation was carried out while under 2 % sodium pentobarbital anesthesia. Following the alleviation of animal suffering during the experiments, the study was approved by the Animal Ethics Committee of Southwest Medical University. An intraperitoneal injection of 150 µg/kg of Rapamycin (RAPA) was administered within 1 h post-surgery. 5 mg of RAPA was dissolved in dimethyl sulfoxide and was kept in a freezer at -20°; RAPA was diluted in Phosphate Buffered Saline (PBS) containing 5 % tween 80 and 5 % polyethlene glycol 400[9].

Animal grouping and treatment:

Rats were randomly divided into 6 groups namely, blank (sham) group containing normal rats; ICH modeling group which were given an equal amount of saline; FYXN Low dose modeling Group (FLG) were given 5 g/kg/d of FYXN; FYXN Medium dose modeling Group (FMG) were given 10 g/kg/d FYXN, FYXN High dose modeling Group (FHG) was given 20 g/kg/d of FYXN and RAPA modeling group was given intraperitoneal injection of 150 µg/kg of RAPA within 1 h after surgery, given the same amount of saline. All the rats were gavaged once/day for 3 d consecutively.

Preparation of ICH model: Anesthetized rats were placed in the prone position and the head was fixed on the brain stereotaxic apparatus. Brain stereotaxic localizer was adjusted in the center of the rat's head to locate to the rat's coronal suture and the periosteum was coated with 3 % hydrogen peroxide, which facilitated to strip the periosteum of the rat. The microsampler tip was placed 1 mm ahead of the fontanel and 3 mm away. A tiny hole, approximately 1 mm wide was drilled on the right side of the midline. A dental drill and a Hamilton 26 gauge syringe needle was inserted into the right deep cortex/basal ganglion at a rate of 1 mm/min in a stereotactic guided manner of 5.5 mm. The needle was stopped for 5 min, adjusted the height of the microsampler and was kept for 10 min. Then, slowly it was pulled out the microsampler, filled the bone wax and incision was sutured. The incision was disinfected with iodine wash and was sterilized with povidone-iodine. 80 000 IU/d of penicillin was injected intramuscularly into each rat to prevent infection. The rats were fed in separate cages after the operation. Except for the blank group, all rats were subjected to the above operation.

Evaluation of brain function: Neurological function assessment was conducted on all animals at 1st and 3rd d of the post modeling. The evaluation involved a series of altered neurologic severity ratings modified Neurological severity score (mNss) that included assessments of motor skills, sensory perception, reflexes and balance, as mentioned earlier. Neurological performance was assessed using a scale ranging from 0-18, with 0 representing normal function and 18 indicating the most severe impairment[10]. Rats with normal scores after modeling were excluded from the groups, remodeled and included in the count.

Histological staining and electron microscopy: Brain tissues were sliced into 4 µm sections treated with xylene to remove paraffin and then dried using alcohol. In the following step, the sections were stained with hematoxylin to visualize the morphology of the brain tissue under a Leica white light microscope (Leica, Germany). Similarly, brain tissues utilized Nissl stain following the same procedure for observation under the microscope.

3 % glutaraldehyde was pre-fixed and 1 % osmium tetroxide was refixed for electron microscopy. After

being dehydrated with acetone, the samples were encased in Epon812, sliced with a diamond blade, dyed with uranyl acetate and lead citrate and was examined using a transmission electron microscope.

Terminal deoxynucleotidyl transferase deoxyUridine triphosphate Nick End Labeling (TUNEL) assay was carried out using a single-step kit (Beyotime, China), following the guidelines. After Deoxyribonucleic Acid (DNA) breakage, sections were labeled with red fluorescent probe for 3'-Hydroxyl (3'-OH) and evaluated under a fluorescent microscope.

Cyberpharmacology: Various databases and platforms were utilized to collect information related to the active ingredients and their respective genes were identified. Cytoscape version 3.10 was used to create a network diagram of TCM-active ingredient-intersecting genes based on comparison with ICH genes from GeneCards. Furthermore, Metascape database was utilized for conducting Gene Ontology (GO) and Kyoto Encyclopedia of Genes and Genomes (KEGG) enrichment analyses based on Protein Protein Interactions (PPI) from the Search Tool for the Retrieval of Interacting Genes/Proteins (STRING) database.

Western blotting: Total protein concentration in the rat brain hematoma was measured using the Bicinchoninic Acid (BCA) protein assay kit (Beyotime, China). Sodium Dodecyl Sulfate-Polyacrylamide Gel Electrophoresis (SDS-PAGE) separated the proteins and transferred them to Poly Vinylidene Fluoride (PVDF) membrane. Following the process of blocking of the membrane using skimmed milk, primary antibodies such as rabbit anti-BECN-1 (Cell Signaling Technology, United States of America (USA), rabbit anti-cleaved caspase-3 (Cell Signaling Technology, USA), rabbit anti-Bcl-2 (Cell Signaling Technology, USA), rabbit anti-BAX (Cell Signaling Technology, USA), rabbit anti-JNK1 (GeneTex, USA) and rabbit anti-autophagic protein microtubule-associated protein 1 Light Chain-3B (LC3B) (Abcam, United Kingdom (UK)) were left to incubate overnight at 4°. Enhanced chemiluminescence was used on 2nd d as a loading control for immunoblotting.

Experiments *in vitro*:

Experimental cells: On d 2, we employed enhanced chemiluminescence for immunoblotting as a loading control. The neurons were seeded in 6-well plates and the study included the groups namely, control group (sham group) which received no treatment; Hemoglobin (Hemin) group which was treated with Hemin for 12 h; FYXN group received both Hemin along with FYXN and RAPA group received Hemin along with RAPA.

Cell Counting Kit-8 (CCK-8) assay: It involves seeding of SH-SY5Y cells in 96-well plates. Cell viability was determined by CCK-8 assay (Biox Technology, USA) and the absorbance was recorded at 450 nm using an enzyme labeling device (Hangzhou Allsheng Instruments, China).

Immunofluorescence double staining: Bcl-2, BAX antibody with Bcl-2 antibody and BECN-1 antibodies were double-stained with each group of cells and observed using a Lycra microscope. Further, TUNEL staining and Western blotting was also performed.

Statistical analysis:

ImageJ 1.53q (National Institute of Health, USA) was used to extract grayscale values and GraphPad Prism version 8.0 (GraphPad Software) was employed for data analysis and creating graphs. The data was presented as mean±Standard Deviation (SD). Analysis of Variance (ANOVA) was used to analyze all the data, with statistical significance defined to be $p<0.05$.

RESULTS AND DISCUSSION

In the experiment, 6 rats died in which 4 died due to anesthesia intolerance while 2 died due to improper modeling. Additionally, 2 rats were excluded from the modeling process as their mNss score screening results did not meet the study criteria. These excluded rats, along with the ones that died, were considered lost and not included in the final experiment. Lost rats were replaced randomly from spare rats. The experimental modeling success rate was approximately 85 % with a corresponding loss rate of about 15 %.

Further, reduction of neurologic deficits after ICH due to FYXN decoction *in vivo* was studied. We evaluated the effects of ICH modeling on neurological function by measuring the mNss on the 1st and 3rd d after drug administration in rats. ICH group had notably higher mNss scores than the control group ($p<0.05$). Furthermore, there were notable variations in mNss scores among all treatment groups when compared to the ICH group ($p<0.05$). When comparing groups pairwise, it was found that the FLG group had significantly lower mNss scores than the ICH group ($p<0.01$), while FMG and FHG groups displayed significantly lower mNss scores compared with

ICH group ($p<0.0001$). Furthermore, FHG group exhibited notably reduced mNss scores compared to the FLG group ($p<0.05$), while the RAPA group showed significantly elevated mNss scores in comparison to the FLG group ($p<0.05$). Moreover, mNss score showed significant increase in RAPA group when compared to the FHG group ($p<0.0001$). These findings suggest that FYXN may have a positive effect on improving the neuronal function in ICH rats, while RAPA as an autophagy agonist does not enhance neurological deficits following cerebral hemorrhage (fig. 1).

Pathological changes attenuated by FYXN after ICH *in vivo* were discussed, where we found that FYXN enhances neurological deficit behavior, which can be detected pathomorphologically. Therefore, we conducted Hematoxylin and Eosin (H&E), Nissl and TUNEL staining including electron microscopy tests.

H&E staining revealed that neurons in sham group exhibited clear and complete characteristics, including full cytosol, clear cytoplasmic staining and tight arrangement. Conversely, ICH group showed high proportion of disordered swollen cells with unclear boundaries, vacuole degeneration and loose interstitium. In FLG and FMG groups, there were still signs of disordered swollen cells, unclear boundaries and loose interstitium. FHG group showed significant decrease in cell gap when compared to the group with cerebral hemorrhage. RAPA group exhibited significant variations in cell spacing, infiltration of inflammatory cells and clear signs of neuron cell death.

Nissl staining results illustrated that the cell structure in sham group was clear, complete, and orderly arranged. In contrast, the cell structure in ICH group was mixed, chaotic in arrangement, swollen, deformed, with nuclear fragmentation and solidification. FLG, FMG and FHG groups exhibited significant improvements compared to the ICH group with more complete cell structure and orderly arrangement as the dosage increased; FHG group showed the most substantial improvement. Conversely, RAPA group exhibited disorganized cell organization and reduced Nissl bodies, which had the most significant effect.

Electron microscopy observations depicted that neurons in sham group had normal morphology, organelles and cell contents without abnormalities as well as visible normal mitochondria. In contrast, neurons in ICH group displayed damaged nuclear membrane integrity, pore formation, content release and high production of mitochondria. FLG, FMG and FHG groups showed significant improvements compared with the ICH group, with relatively intact nuclear structure, reduced nuclear solidification and decreased mitochondria. Meanwhile, RAPA group exhibited a noticeable improvement, with high production of mitochondria and autophagosomes. FHG group displayed a particularly substantial enhancement with better nuclear and mitochondrial conditions.

CCK-8 detection of drug concentration was carried out. By default, the cell viability of the sham group was found to be 1. The cell activity of SH-SY5Y was reduced under the influence of hemosiderin, and the cell activity was close to 50 % after 12 h of treatment with 100 μM ($p<0.05$). Therefore, a concentration of 100 μM Hemin was chosen to treat cells for 12 h to simulate an *in vitro* ICH model in the subsequent experiments.

The cell activity of SH-SY5Y cells increased after Hemin group under the influence of 2 % Fuzen to wake up brain was used to treat SH-SY5Y cells following Hemin group. The cell activity was highest at 200 nM RAPA+Hemin for 12 h ($p<0.05$). Therefore, SH-SY5Y cells treated with 2 % concentration of Hemin to simulate the Fuzen wakeup brain treatment model for 12 h in the subsequent experiments.

After SH-SY5Y cells were modeled with ferroportin, cell activity decreased under the influence of RAPA and the cell activity was highest when treated with 200 nM of RAPA+Hemin for 12 h ($p<0.05$). Therefore, SH-SY5Y cells treated with 200 nM RAPA under the influence of Hemin for 12 h were chosen to simulate the RAPA treatment model in the subsequent experiments (fig. 2).

Then we found out that FYXN decreases cell death following ICH both in live organisms and in laboratory experiments. Enhanced tissue structure post ICH indicates that FYXN could potentially mitigate the pathological harm caused by ICH. To investigate whether FYXN can effectively reduce apoptosis, TUNEL fluorescence staining was performed to assess the survival proportion in tissues and cells. *In vivo* experiments showed high number of TUNEL-positive cells in the ICH group, while the apoptosis rate in the FMG and FHG groups decreased significantly compared to the ICH group ($p<0.05$). Additionally, there was a notable decrease in the rate of apoptosis in the FMG and FHG groups when

compared with the FLG group ($p<0.05$). Conversely, RAPA group displayed a notable increase in TUNEL-positive cells, with a significantly higher apoptotic rate compared to both the ICH group and the FYXN groups ($p<0.05$). The rate of apoptosis was notably higher ($p<0.05$) when compared to both the ICH and FYXN groups.

Both the *in vivo* and *in vitro* results showed consistency, with a noticeable number of TUNEL-positive cells in the Hemin group leading to a higher apoptotic rate compared to the sham group ($p<0.05$). Conversely, the FYXN group denoted decrease in TUNEL-positive and apoptotic cells in comparison to the Hemin group, with a significance level of $p<0.05$. RAPA group showed a notable amount of TUNEL-positive cells, resulting in a significantly greater rate of apoptosis compared to the Hemin and FYXN groups ($p<0.05$). Overall, FYXN appears to enhance apoptosis after ICH, and increased autophagy does not alleviate apoptosis following ICH.

To investigate the mechanism of FYXN on ICH, FYXN and ICH disease genes were intersected and imported into STRING to obtain a PPI network analysis. The data was further analyzed using Cytoscape version 3.10 to create a map showing the intersection of FYXN Chinese medicine-active ingredient-intersected genes. Additionally, FYXN was intersected with ICH disease genes and imported into Metascape to obtain GO enrichment bar graphs and KEGG enrichment bubble graphs. Neurology-related pathways were then screened, with a focus on JNK/Bcl-2.

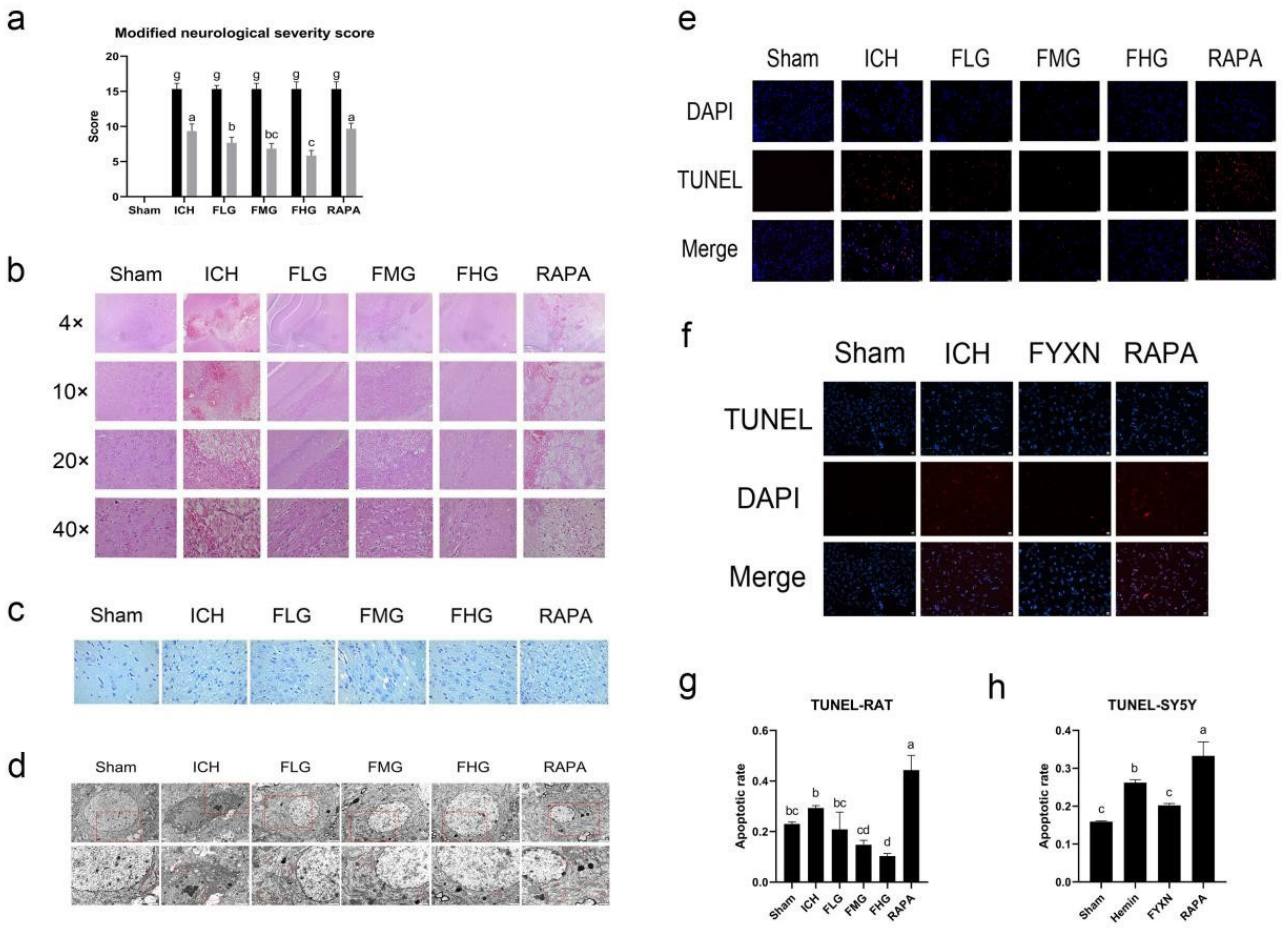

Fig. 1: (a): Altered neurological severity scores of rats at 1 h and 72 h; (b): H&E staining assay was conducted at 40X, 100X, 200X and 400X magnification; (c): Nissl staining (400X); (d): Electron microscopy of cell contents (8000X and 15 000X); (e): *In vivo* TUNEL fluorescence staining results; (f): *In vitro* TUNEL fluorescence staining results (400X); (g): Rate of apoptosis of ICH and FYXN groups and (h): Rate of apoptosis of Hemin and FYXN groups
Note: n=3 and $p<0.05$, (a) (■): 1 h and (■): 72 h

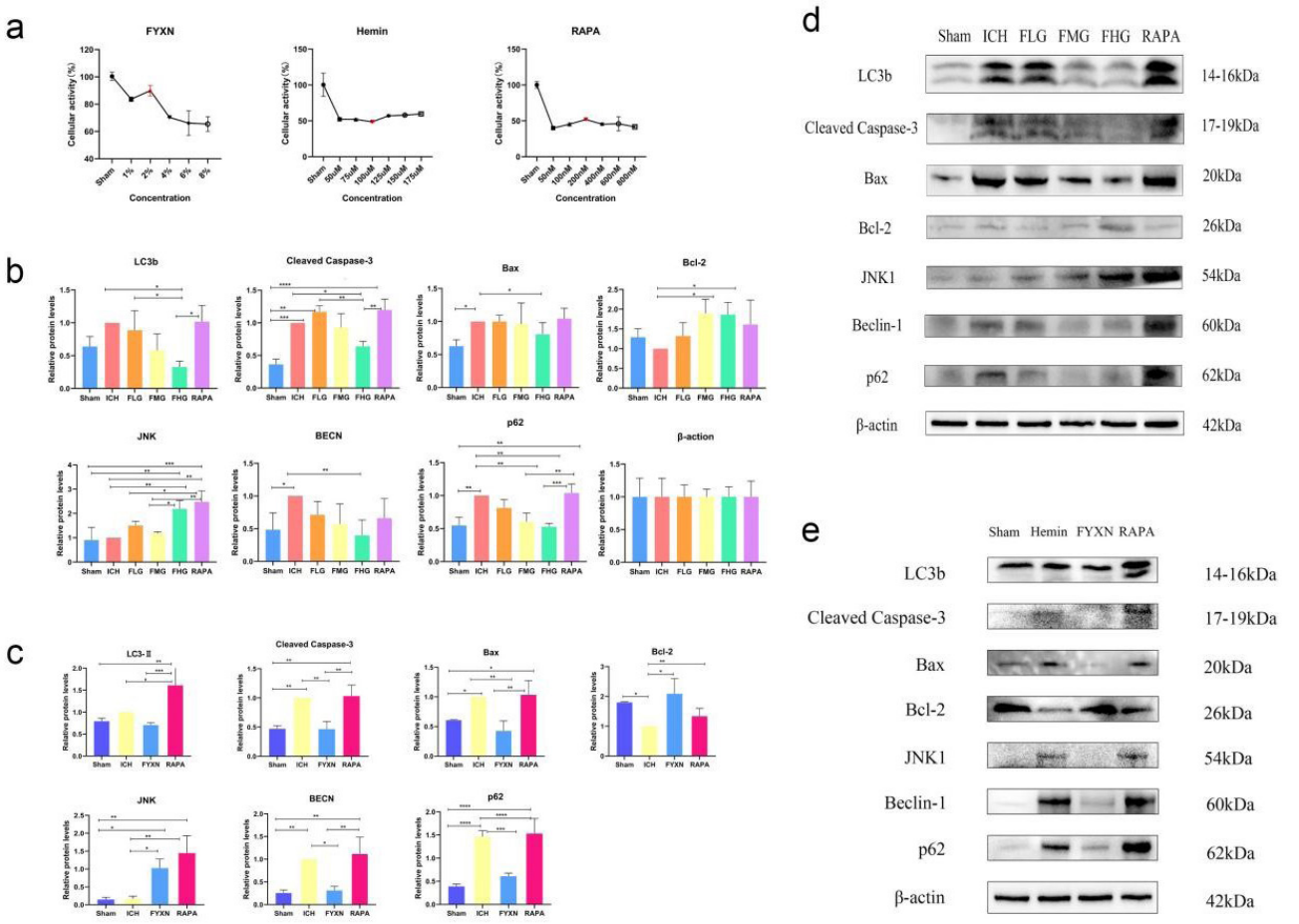

Fig. 2: CCK-8 detection. (a): Hemin, FYXN and rapamycin groups; (b): Expression levels of proteins related to autophagy and cell death after the effect of FYXN on ICH under *in vivo*; (c): Expression levels of proteins related to autophagy and cell death after the effect of FYXN on ICH *in vitro*; (d): Level of autophagy- and death-related protein expression after the effect of FYXN on ICH *in vivo* and (e): Level of autophagy- and death-related protein expression after the effect of FYXN on SH-SY5Y cells *in vitro*

Western blot tests were conducted in both living organisms and in a controlled environment. ICH rats showed significantly elevated expression levels of BAX, cleaved caspase-3, BECN and sequestosome 1 (p62) proteins compared to the control group ($p<0.05$). Nevertheless, FHG group exhibited notably reduced expression levels compared with the ICH group ($p<0.05$). FHG group showed significantly lower levels of cleaved caspase-3, BECN-1, LC3B and p62 proteins compared to the FLG group ($p<0.05$). JNK expression levels were markedly elevated in RAPA group compared with the ICH group. Moreover, RAPA group exhibited notably elevated levels of cleaved caspase-3, LC3B and p62 proteins compared with ICH group ($p<0.05$) (fig. 3).

BAX, cleaved caspase-3, BECN-1 and p62 levels were notably higher in SH-SY5Y cells treated with Hemin compared with the sham group ($p<0.05$), while they were lower in Bcl-2 group ($p<0.05$). In contrast to the Hemin group, SH-SY5Y cells in FYXN group exhibited notably reduced levels of BAX, cleaved caspase-3, BECN-1 and p62 protein expressions ($p<0.05$) with significant increase in Bcl-2 and JNK protein expressions ($p<0.05$).

Within the RAPA group, levels of Bcl-2, LC3B and JNK proteins showed a notable increase in SH-SY5Y cells when compared with Hemin group ($p<0.05$). Moreover, compared with the FYXN group, the expression levels of BAX, cleaved caspase-3, LC3B and BECN-1 were increased in the RAPA group in SH-SY5Y cells ($p<0.05$).

It was also found that FYXN regulates the ratio and distribution of Bcl-2 to BAX and BECN-1 by regulating Bcl-2. In order to develop deeper into the accumulation and ratio of Bcl-2, BAX and BECN-1 after ICH, SH-SY5Y cells were simultaneously stained with BAX and Bcl-2, along with BECN-1 and Bcl-2 (fig. 4). The double-staining results for

Bcl-2/BAX showed low Bcl-2 levels and high BAX levels in Hemin group, resulting in a significantly lower Bcl-2/BAX ratio compared to the sham group ($p<0.05$). Moreover, the FYXN group showed elevated levels of Bcl-2 and low levels of BAX, resulting in a notable reduction in the Bcl-2/BAX ratio when compared to the sham group.

Moreover, Bcl-2/BAX dual staining revealed a decrease in Bcl-2 levels and an increase in BAX levels in the Hemin group, leading to a significant reduction in the Bcl-2/BAX ratio compared to the sham group ($p<0.05$). Within the FYXN group, there was notable upregulation of the Bcl-2/BAX ratio compared with sham and Hemin groups, with both Bcl-2 and BAX ($p<0.05$). Conversely, RAPA group exhibited distinct expression levels of Bcl-2 and BAX, resulting in a notable reduction in the Bcl-2/BAX ratio when compared to the sham, Hemin and FYXN groups ($p<0.05$).

Bcl-2 and BECN-1 expression levels were significantly higher in Hemin group compared to the sham group ($p<0.05$) in Bcl-2-BECN-1 co-staining. Conversely, in the FYXN group, Bcl-2 and BECN-1 were expressed separately with no fluorescence overlapping, leading to an elevated Bcl-2/BECN-1 ratio compared to the Hemin group. Additionally, RAPA group showed higher levels of Bcl-2 and BECN-1 expression when compared with sham, Hemin and FYXN groups ($p<0.05$).

RAPA group exhibited higher BECN-1 expression than the FYXN group, with BECN-1 levels surpassing those of Bcl-2 and notably reduced Bcl-2/BECN-1 ratio in Hemin and FYXN groups ($p<0.05$). The findings along with the protein imprinting outcomes of Bcl-2, BAX and BECN-1 in the Western blot test indicate that FYXN could control autophagy and apoptosis post ICH by adjusting the connections among Bcl-2, BAX and BECN-1.

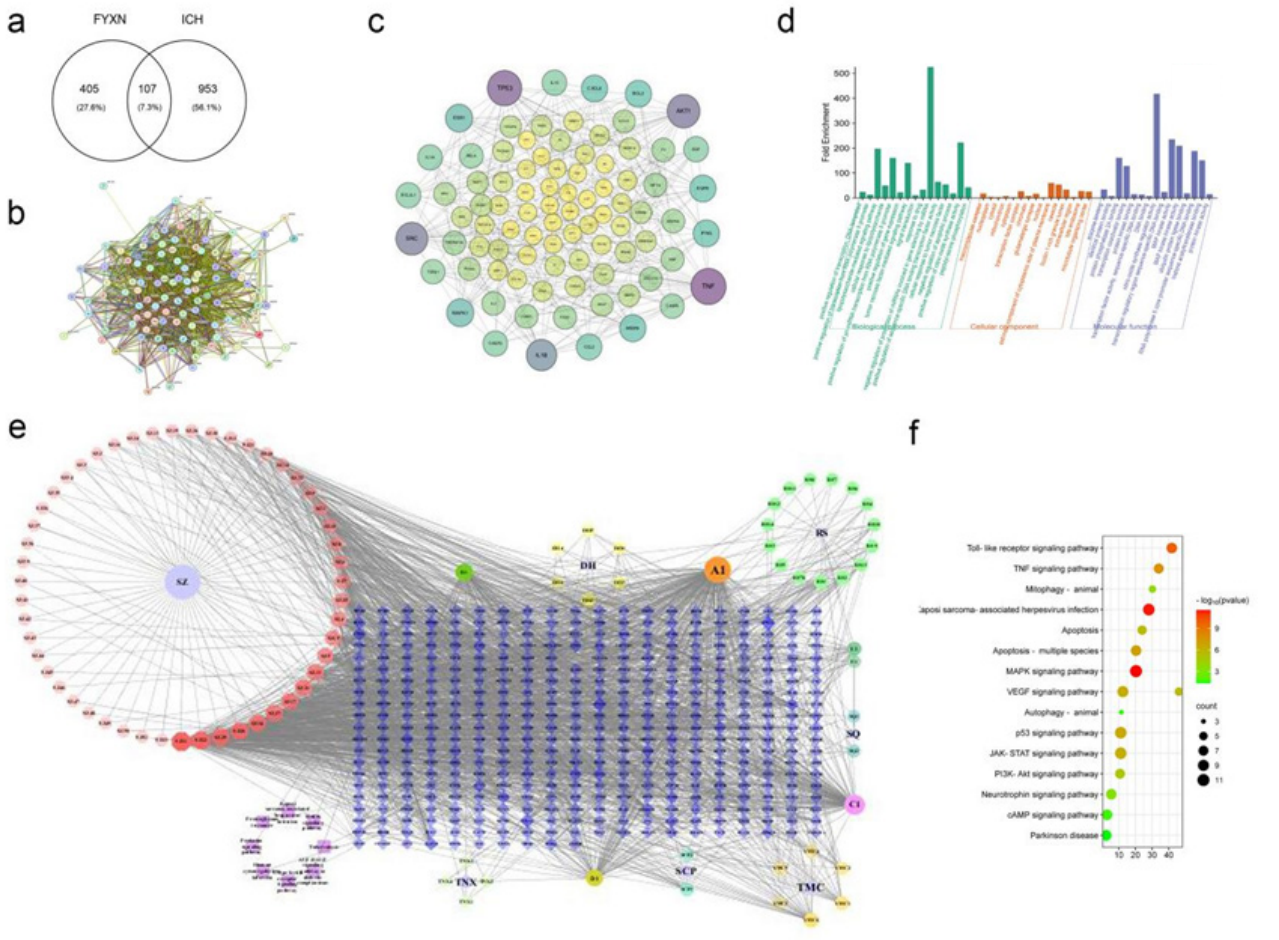

Fig. 3: (a): FYXN-ICH Venn diagram (b): PPI network analysis plot; (c): PPI analysis of intersecting genes; (d): GO enrichment analysis; (e): FYXN Chinese herbal medicine-active ingredient intersecting genes analysis and (f): KEGG enrichment analysis
Note: (d) (▬): Biological process; (▬): Cell Components (CC) and (▬): Molecular Function (MF)

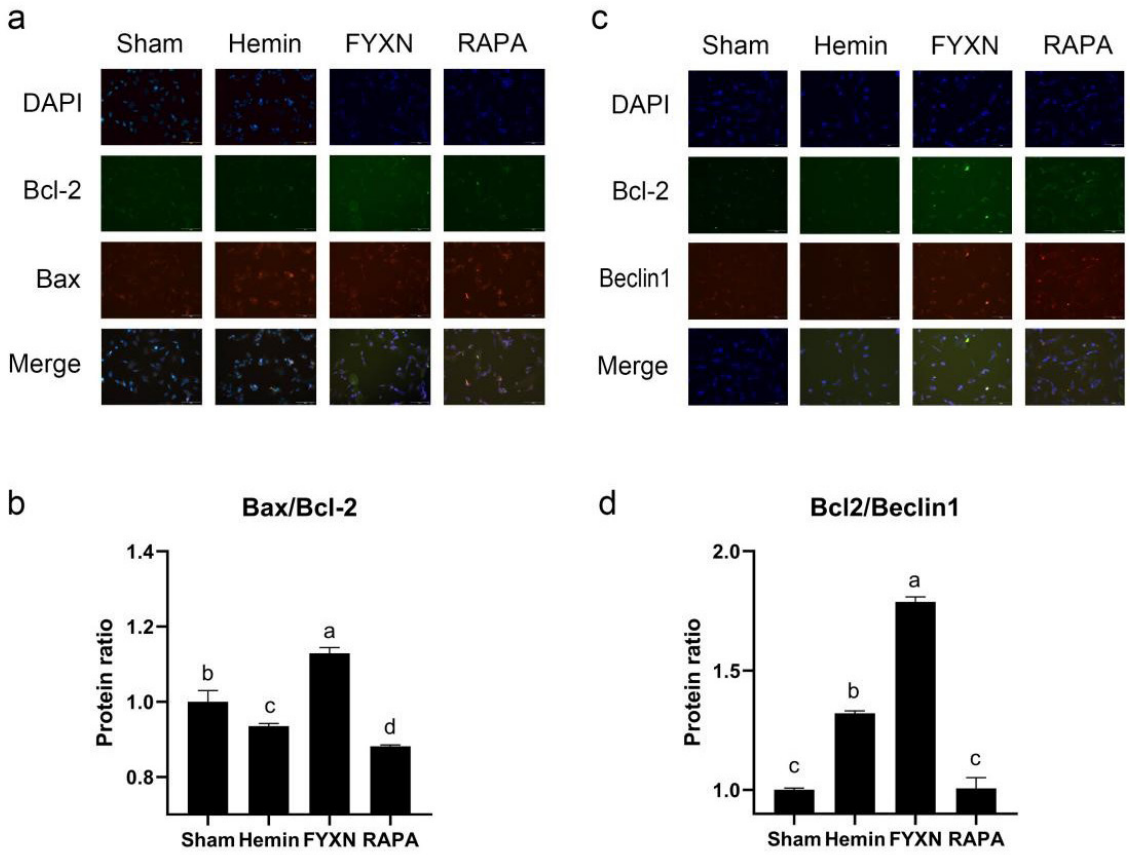

Fig. 4: Double staining immunofluorescence. (a): Bcl-2-BAX; (b): Bcl-2-BECN-1; (c): Quantitative analysis of immunofluorescence to determine the Bcl-2/BAX ratio and (d): Analysis of Bcl-2/BECN-1 ratio using quantitative immunofluorescence
Note: n=3 and p<0.05

BAX/Bcl-2 ratio which is an important marker of cell death is strongly linked to the speed at which cells undergo apoptosis[11,12]. It also correlates partially with the disease site and serves as a potential molecular marker for certain cancers[13]. Bcl-2, known for its role in preventing apoptosis, also interacts with BECN-1 to inhibit the initiation of autophagy. The regulation whether to block apoptosis or autophagy appears to involve a competitive process. However, when the levels of Bcl-2 are elevated, this competition is resolved, highlighting the crucial regulatory role of Bcl-2. Higher expression levels of FHBcl-2 and JNK were observed in FYXN group compared to the ICH group in both *in vivo* and *in vitro* experiments. Furthermore, a certain degree of association between JNK and Bcl-2 was noted. Previous experiments have confirmed the relevance of the JNK/Bcl-2 interaction to autophagic diseases in the brain. Overall, these findings suggest that Bcl-2 plays a key regulatory role in determining the balance between apoptosis and autophagy. The results of the experiments shed light on the intricate association between JNK and Bcl-2, emphasizing their significance in the context of autophagy-related diseases in the brain[14,15]. FYXN may play a crucial role in reducing the occurrence of autophagy and apoptosis following ICH through the JNK/Bcl-2 pathway. It appears that FYXN contributes to the decrease in autophagy and apoptosis post-ICH *via* the JNK/Bcl-2 pathway. However, whether FYXN can prevent apoptosis while inhibiting autophagy or apoptosis by inhibiting autophagy is still unsolved, as autophagy and apoptosis seem to be engaged in a competitive relationship[16]. Increased autophagy may decrease apoptosis; however, ICH demonstrates increased apoptosis in the presence of autophagy agonists. Excessive autophagy has been observed in an *in vivo* ICH model treated with RAPA. It has been previously concluded that excessive autophagy ultimately leads to increased cell death[17].The present study has some limitations as autophagy agonists were not co-administered with FYXN in the experimental subjects, and there is limited evidence that FYXN decreases autophagy. Additionally, FYXN contains a variety of compounds that have shown benefits in the treatment of stroke. Thus, further exploration of

the combined effects of these compounds on stroke is necessary.

Author's contributions:

Moyan Wang is the first author while Xue Bai and Bangjiang Fang contributed equally as corresponding authors. All authors have read and approved the final manuscript.

Funding:

This study was supported by Innovation Team and Talents Cultivation Program of National Administration of Traditional Chinese Medicine (Grant No: ZYYCXTD-C-202207); Sichuan Science and Technology Program (Grant No: 2022YFS0613); Luzhou Science and Technology Program (Grant No: 2020-SYF-30) and Program of Southwest Medical University (Grant No: 2023ZYYJ01; 2023ZYYJ09; 2020XYLH-018 and 2020XYLH-029).

Conflict of interests:

The authors declared no conflict of interests.

REFERENCES

1. Schrag M, Kirshner H. Management of intracerebral hemorrhage: JACC focus seminar. J Am Coll Cardiol 2020;75(15):1819-31.
2. Shao A, Zhu Z, Li L, Zhang S, Zhang J. Emerging therapeutic targets associated with the immune system in patients with Intracerebral Haemorrhage (ICH): From mechanisms to translation. EBioMedicine 2019;45:615-23.
3. Duan XC, Wang W, Feng DX, Yin J, Zuo G, Chen DD, *et al*. Roles of autophagy and endoplasmic reticulum stress in intracerebral hemorrhage-induced secondary brain injury in rats. CNS Neurosci Ther 2017;23(7):554-66.
4. Jiang C, Wang T, Ma Z. Effectiveness of Fuyuan Xingnao decoction for patients with diabetes mellitus combined cerebral infarction: Erratum. Medicine 2019;98(44):1-8.
5. Jiang C, Wang T, Ma Z, Fang BJ. Effectiveness of Fuyuan Xingnao decoction for patients with diabetes mellitus combined cerebral infarction. Medicine 2019;98(39):1-17.
6. Bekker M, Abrahams S, Loos B, Bardien S. Can the interplay between autophagy and apoptosis be targeted as a novel therapy for Parkinson's disease? Neurobiol Aging 2021;100:91-105.
7. Chiu CH, Ramesh S, Liao PH, Kuo WW, Chen MC, Kuo CH, *et al*. Phosphorylation of Bcl-2 by JNK confers gemcitabine resistance in lung cancer cells by reducing autophagy-mediated cell death. Environ Toxicol 2023;38(9):2121-31.
8. Deng D, Qu Y, Sun L, Jia L, Bu J, Ye M, *et al*. Fuyuan Xingnao decoction promotes angiogenesis through the Rab1/AT1R pathway in diabetes mellitus complicated with cerebral infarction. Front Pharmacol 2021;12:1-16.
9. Lu Q, Gao L, Huang L, Ruan L, Yang J, Huang W, *et al*. Inhibition of mammalian target of rapamycin improves neurobehavioral deficit and modulates immune response after intracerebral hemorrhage in rat. J Neuroinflammation 2014;11:1-14.
10. Li X, Zhang D, Bai Y, Xiao J, Jiao H, He R. Ginaton improves neurological function in ischemic stroke rats *via* inducing autophagy and maintaining mitochondrial homeostasis. Neuropsychiatr Dis Treat 2019;15:1813-22.
11. Salavatipour MS, Kouhbananinejad SM, Lashkari M, Bardsiri MS, Moghadari M, Kashani B, *et al*. Kermanian propolis induces apoptosis through upregulation of BAX/Bcl-2 ratio in acute myeloblastic leukemia cell line (NB4). J Cancer Res Ther 2023;19(2):327-34.
12. Masoud M, Maryam SS, Mahla SB, Mehrnaz KS, Mahla L, Reza V, *et al*. Elevated BAX/Bcl-2 ratio: A cytotoxic mode of action of kermanian propolis against an acute lymphoblastic leukemia cell line, NALM-6. Indian J Hematol Blood Transfus 2022;38(4):649-57.
13. Khodapasand E, Jafarzadeh N, Farrokhi F, Kamalidehghan B, Houshmand M. Is BAX/Bcl-2 ratio considered as a prognostic marker with age and tumor location in colorectal cancer? Iran Biomed J 2015;19(2):69-75.
14. Zhang S, Gui XH, Huang LP, Deng MZ, Fang RM, Ke XH, *et al*. Neuroprotective effects of β-asarone against 6-hydroxy dopamine-induced parkinsonism *via* JNK/Bcl-2/beclin-1 pathway. Mol Neurobiol 2016;53(1):83-94.
15. Liu L, Fang YQ, Xue ZF, He YP, Fang RM, Li L. Beta-asarone attenuates ischemia-reperfusion-induced autophagy in rat brains *via* modulating JNK, p-JNK, Bcl-2 and beclin 1. Eur J Pharmacol 2012;680(1-3):34-40.
16. Kroemer G, Mariño G, Levine B. Autophagy and the integrated stress response. Mol Cell 2010;40(2):280-93.
17. Fricker M, Tolkovsky AM, Borutaite V, Coleman M, Brown GC. Neuronal cell death. Physiol Rev 2018;98(2):813-80.

This article was originally published in a special issue, "Clinical Advancements in Life Sciences and Pharmaceutical Research" Indian J Pharm Sci 2024:86(5) Spl Issue "18-26"